

# High resolution solid state NMR spectroscopy in surface organometallic chemistry: access to molecular understanding of active sites of well-defined heterogeneous catalysts

Frédéric Blanc,<sup>a</sup> Christophe Copéret,<sup>\*a</sup> Anne Lesage<sup>b</sup> and Lyndon Emsley<sup>\*b</sup>

Received 7th October 2007

First published as an Advance Article on the web 5th November 2007

DOI: 10.1039/b612793m

Recent advances in solid state NMR spectroscopy have made possible the understanding of surface species and active sites of heterogeneous catalysts at a molecular level. This *tutorial review* describes solid state NMR spectroscopy, what are the possible techniques to obtain high resolution and 2D spectra (structural information), and what are their applications in the context of well-defined heterogeneous catalysts prepared by surface organometallic chemistry.

<sup>a</sup>Université de Lyon, Institut de Chimie de Lyon, LC2P2-CNRS, Equipe Chimie Organométallique de Surface, CPE Lyon, 43 bd du 11 Novembre 1918, F-69616 Villeurbanne Cedex, France. E-mail: coperet@cpe.fr; Fax: (+33)4-7243-1795; Tel: (+33)4-7243-1811

<sup>b</sup>Laboratoire de Chimie (UMR 5532), ENS Lyon, 46 Allée d'Italie, F-69364 Lyon Cedex 07, France. E-mail: lyndon.emsley@ens-lyon.fr; Fax: (+33)4-7272-8483; Tel: (+33)4-7272-8486



Left to right: Christophe Copéret, Lyndon Emsley, Frédéric Blanc and Anne Lesage

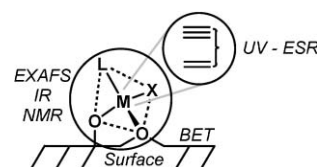
Lyndon Emsley, Anne Lesage and Christophe Copéret have been working together on the development of NMR methods for the understanding of well-defined heterogeneous catalysts since 1999; Frédéric Blanc joined the team as a joint PhD student in 2004 and recently graduated (October 2007). More specifically, Lyndon and Anne have been developing new NMR methods for the study of the structure and dynamics of a wide range of solid-state compounds at the Chemistry Department of the Ecole Normale Supérieure de Lyon (ENS Lyon), and Christophe's research interest has been focusing on the molecular understanding of the surface chemistry of oxides and metals, more particularly in the area of heterogeneous catalysis in the Laboratoire de Chimie Organométallique de Surface of the Ecole de Chimie de Lyon (CPE Lyon).

## 1. Introduction

In the search for more efficient chemical processes, one key approach consists in the development of more selective and more active heterogeneous catalysts. Improving these complex systems in a rational way can be undertaken through the powerful structure–reactivity approach, but this requires a precise molecular understanding of the active sites.<sup>1</sup> This approach has been called surface organometallic chemistry (SOMC), and one of its goals is to develop and use new tools to characterize active sites at a molecular level (Scheme 1). Spectroscopic methods<sup>2</sup> are particularly interesting because they can provide information on the electronic states and the structures of the active sites, which in turn provide molecular information and allow a possible rational improvement of the catalysts. Within this goal, infrared (IR), Raman, solid state NMR, UV-Vis and X-ray absorption (XAS) spectroscopies along with other surface science techniques and molecular modelling have been extensively used. We will review the recent advances in solid state NMR spectroscopy applied to the understanding of the active sites of heterogeneous catalysts, using selected examples. We will first briefly discuss the basics of solid state NMR spectroscopy,<sup>3</sup> and then the more recent developments of the methods and their application to the characterization of well-defined heterogeneous catalysts.

## 2. Basic principles of solid state NMR

We first briefly discuss the fundamentals of NMR in general, and the specificity of solid state NMR in particular. Chemists mainly rely on chemical shifts  $\delta$  and scalar  $J$  couplings to



**Scheme 1** General strategy to understand structures of surface complexes.

resolve the structure of complex molecules, and these data are readily available in solution state NMR. For powdered solids, these parameters are largely hidden because of the presence of large anisotropic interactions like dipolar couplings and chemical shift anisotropies, which lead to a significant broadening of the signals (0–50 kHz, value to be compared with 0–5 kHz and 0–200 Hz for  $\delta$  and  $J$  values, respectively).<sup>3</sup>

Indeed, for spins  $I = \frac{1}{2}$  the Hamiltonian can be expressed as follows (eqn 1):

$$H = H_z + H_{cs} + H_j + H_d \quad (1)$$

where  $H_z = -\gamma_j B_o \hat{I}_j$  represents the Zeeman interaction of the nuclear spin with the applied magnetic field,  $H_{cs} = \gamma_j \sigma_j B_o \hat{I}_j$  the chemical shift interaction arising from the induced magnetic field by electrons,  $H_j = \hat{I}_j \cdot J_{jk} \cdot \hat{I}_k$  the scalar  $J$  coupling interaction between bonded nuclei and  $H_d$  the dipolar coupling interaction of each nuclear spin. In the case of homonuclear coupling (between like spins), the dipolar interaction is  $H_d = d_{jk} \left( 3 \hat{I}_{jz} \hat{I}_{kz} - \vec{I}_j \cdot \vec{I}_k \right)$  whereas the expression is simplified to  $H_d = d_{jk} 2 \hat{I}_{jz} \hat{I}_{kz}$  for heteronuclear coupling. Both the chemical shift Hamiltonian and the dipolar coupling Hamiltonian depend on the orientation of the molecule with respect to the direction of the external field. Typically, in powdered solids, the sample contains many crystallites with random orientations, and the anisotropic interactions thus lead to powder patterns, since all the different molecular orientations present in the sample give rise to different spectral frequencies.<sup>3a,3b</sup> The resulting lack of resolution obscures the information contained in the spectrum. It is thus necessary to apply special techniques to obtain high resolution spectra. This is in major contrast with liquid state NMR, for which fast tumbling of molecules causes the anisotropic interactions to average themselves to isotropic values resulting in sharp lines. This situation is summarized in Fig. 1.

In the solid state, the frequency of a particular crystallite is spatially dependent, but all the interactions have the same

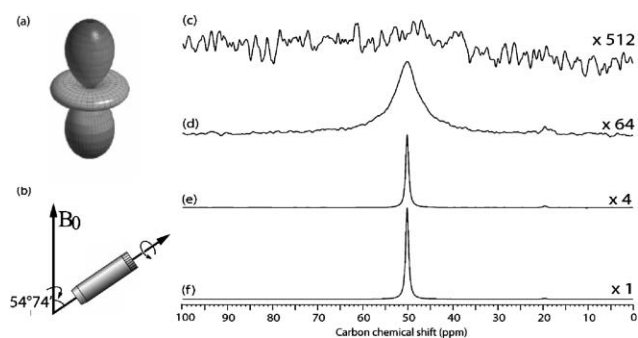


**Fig. 1** Schematic representation of the (a) the angular dependence of an anisotropic interaction and (b) a rotor at the magic angle. (c, d, e & f) one dimensional (1D)  $^{13}\text{C}$  spectra of  $[2-^{13}\text{C}]$  alanine. (c) Static spectrum. (d) Spectrum recorded spinning the sample at 30 kHz at the magic angle. (e) Spectrum under magic angle spinning (MAS) at 12.5 kHz and heteronuclear decoupling during acquisition (100 kHz). (f) Spectrum under magic angle spinning (MAS) at 12.5 kHz, cross polarization  $^1\text{H}$ - $^{13}\text{C}$  and heteronuclear decoupling during acquisition (100 kHz).

“second rank” spatial dependence, and we find notably that (eqn 2):

$$\omega \propto \frac{1}{2} (3 \cos^2 \theta - 1) \quad (2)$$

with  $\theta$  = the angle between the principal axis of the interaction tensor and the static magnetic field  $B_o$ . This spatial dependence can be exploited to our advantage. It was shown in the pioneering works in the late fifties of Andrew and Eades<sup>4</sup> and of Lowe<sup>5</sup> that the anisotropic broadening can be averaged to zero when the sample physically rotates around  $\theta = 54.74^\circ$ . This angle is referred to as the “magic angle” ( $\theta_m$ ) since the resulting spectrum has the similar narrow lines characteristics (in principle) to a liquid-state spectrum. The associated technique, known as magic angle spinning (MAS) (Fig. 1a and b), has been extensively used in solid state NMR experiments, with spinning rates routinely set to 10–30 kHz and with up to 70 KHz available commercially today. When the sample is spun around the magic angle at a rate faster than the anisotropy of the interaction, all the crystallites appear to have the same orientation, and at  $\theta_m$  the chemical shift anisotropy and the dipolar interactions are averaged to zero, and thus a reduction of the line broadening is observed. (Unfortunately, the technique is not perfect, and for example carbon-13 linewidths are rarely less than about 50 Hz in the solid state.)

Additionally, it is possible to improve the sensitivity of spectra of low abundance X nuclei such as  $^{13}\text{C}$ ,  $^{15}\text{N}$  or  $^{29}\text{Si}$  by increasing the signal through the transfer of the magnetisation from abundant protons to the X nucleus (similar to the INEPT family of techniques for solution state NMR). In solids, this technique is known as cross polarisation (CP),<sup>6</sup> which is optimal under certain radiofrequency field conditions, known as the Hartmann–Hahn matching conditions (eqn 3):

$$\gamma_H B_1(^1\text{H}) = \gamma_X B_1(\text{X}) \pm n\omega_r \quad (3)$$

where  $\gamma_I$ ,  $B_1(I)$ ,  $n$  and  $\omega_r$  are respectively the gyromagnetic ratio, the spin lock field of spin  $I$ , an integer number and the MAS rate. The results of cross-polarization are shown in Fig. 1. Combining CP and MAS techniques<sup>5</sup> is therefore ideal to obtain high-resolution high sensitivity purely isotropic spectra for low abundance X nuclei, and this has been extensively used to characterize solids including heterogeneous catalysts.<sup>7</sup> Note, however, that this technique is not quantitative, unless CP kinetics are performed,<sup>8</sup> and thus should be used with precaution if one wants to determine the respective amount of several types of a given nuclei, e.g.  $^{13}\text{C}$ . This can be achieved by quantitative single pulse spectra. In a similar way,  $^{31}\text{P}$  can also be used as a polarization source in organometallic and organic phosphorus containing products.<sup>9</sup>

Finally, in solids, the presence of dense networks of naturally abundant nuclei, usually protons, is often the case. Their interactions generate strong couplings (homonuclear couplings, between pairs of identical spins typically protons, or heteronuclear couplings, between  $^1\text{H}$  and  $^{13}\text{C}$ ,  $^{15}\text{N}$ ,  $^{29}\text{Si}$  or  $^{31}\text{P}$ ). This is a source of spectral broadening (Fig. 1), which cannot be fully averaged out by MAS. Therefore, additional methods involving homo-<sup>10</sup> or heteronuclear-<sup>11</sup> decoupling with radiofrequency pulse sequences are required to improve the NMR

spectra by averaging out the residual dipolar interactions even under MAS. In summary, the elements magic angle spinning, cross-polarisation and heteronuclear decoupling combine to form the workhorse solid-state NMR experiment, dubbed simply CP-MAS.

Because the active sites of many catalytic reactions (olefin polymerization, olefin metathesis, alkyne metathesis, hydrogenation...) involve metal–hydrogen (M–H) or metal–carbon bonds (M–C, M=C and M=C), efforts have been made to observe these catalytically active hydrogen and carbon sites in various surface organometallic complexes using for instance simple  $^1\text{H}$  MAS and  $^{13}\text{C}$  CP MAS. However due to the low concentration of active site and low sensitivity of NMR spectroscopy, carbon-13 enriched complexes are typically used to enhance the signal to noise ratio.<sup>7,12</sup>

1D NMR methods are in fact widely used to characterize heterogeneous catalysts.<sup>13</sup> We remark that determining structures by using only chemical shifts can be misleading. Indeed, in liquid-state NMR a plethora of multi-dimensional NMR techniques are routinely used to avoid ambiguities in characterisation. In this review we will discuss the implementation of two-dimensional techniques as well as ways to improve resolution in spectra, in order to confirm the interpretation of spectra.

### 3. High resolution $^1\text{H}$ NMR spectra of surface species

While  $^1\text{H}$  NMR spectroscopy is a crucial tool for structure determination of molecules in solution, the  $^1\text{H}$  spectra in solids are usually broad (typically 40 kHz in a static sample). This is mainly due to the very strong dipolar coupling interactions as a result of a dense network of  $^1\text{H}$  spins. Access to  $^1\text{H}$  chemical shifts is therefore challenging in complex molecular systems, where fast spinning of the sample at the magic angle alone may not always be efficient enough to fully average the anisotropic interactions and to obtain chemical shift information. For instance, proton linewidths of 3 ppm can be achieved at fast MAS frequencies (40 kHz) for organic molecules.<sup>14</sup> This may be sufficient in some cases (notably hydrogen-bonded protons shifted to low field),<sup>15</sup> but is often not enough. An additional increase in resolution can be obtained by combining MAS with the application of homonuclear decoupling sequences. In many cases, the  $^1\text{H}$  NMR spectra of grafted molecules on a surface are sufficiently resolved under MAS alone because many of these surface species covalently linked to the surface have several degrees of motional freedom, which partially average out the dipolar interactions and narrow the lines. Moreover, these systems, and especially the single-site catalysts prepared by SOMC, are usually isolated and dispersed on a support (silica, alumina ...) free of protons, which reduces the proton density at a given site.

For example, the single pulse  $^1\text{H}$  NMR spectrum of  $[(\text{SiO})\text{Mo}(\text{=NAr})(\text{=CH}t\text{Bu})(\text{CH}_2t\text{Bu})]$  shown in Fig. 2a is already well-resolved with rather narrow proton linewidths of around 0.5 ppm at a MAS frequency of 10 kHz.<sup>16</sup> The observed residual broadening is here assigned to both chemical shift distributions (corresponding to a continuum of very slightly different molecular surface structures) and to residual anisotropic interactions. Similar observations are routinely

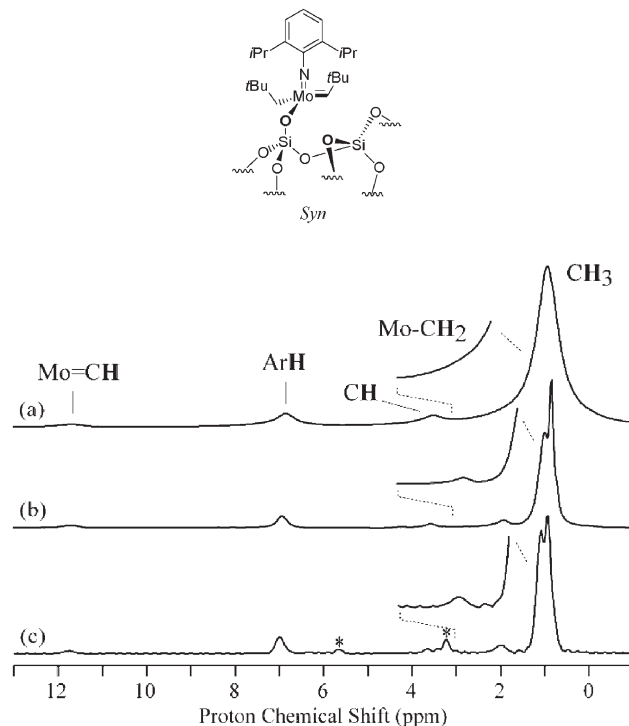
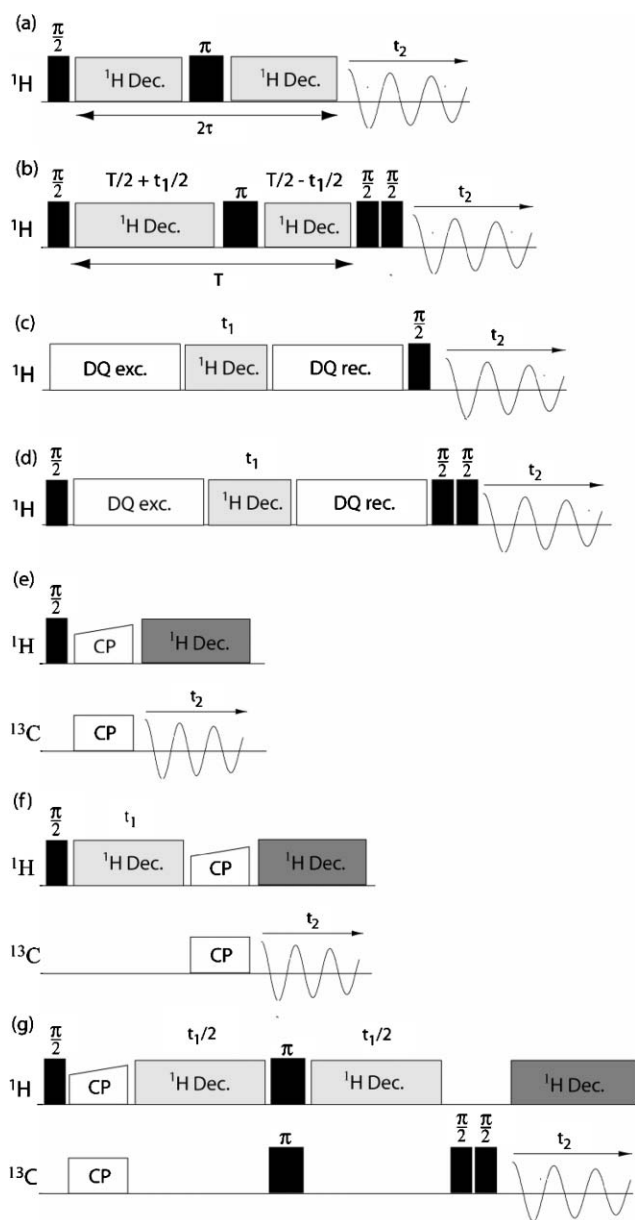


**Fig. 2** Molecular structure and one dimensional  $^1\text{H}$  MAS spectra of  $[\text{syn}-(\text{=SiO})\text{Mo}(\text{=NAr})(\text{=CH}t\text{Bu})(\text{CH}_2t\text{Bu})]$ .<sup>16,17</sup> (a) Single-pulse spectrum. (b) Delayed acquisition spectrum using an echo period. (c) Constant-time spectrum reconstructed from the 2D spectrum. Asterisk (\*) indicates small artefacts present in the 2D spectrum. Adapted with permission from the authors.<sup>16,17</sup>

observed for the hydroxyl groups of silica or alumina for the reason described above (low proton density). While in this sample, faster MAS (up to 30 kHz) does not help to improve the resolution of the single pulse  $^1\text{H}$  spectra,<sup>17</sup> a slight, but significant, improvement in resolution was observed by applying DUMBO homonuclear dipolar decoupling<sup>18,19</sup> during the acquisition of the  $^1\text{H}$  spectrum: for example the linewidth of the methylene  $\text{CH}_2$  proton of the neopentyl ligand being thus reduced in that case by 30%.<sup>16</sup> The application of relatively simple delayed acquisition methods,<sup>20,21</sup> namely echo and constant time acquisition approaches as illustrated in Fig. 2b and 2c, has an even better effect on the improvement of spectral resolution of surface organometallic catalysts (*ca.* by up to a factor of 3).<sup>17</sup>

The spin echo experiment consists of a  $90^\circ$  proton pulse followed by a  $\tau$  delay, a  $180^\circ$  proton pulse and another  $\tau$  delay before direct acquisition of the signal (Scheme 2a). The  $180^\circ$  pulse refocuses the chemical shift distribution and the refocusable terms of the residual dipolar coupling, but some of the crystallite orientations corresponding to the most strongly coupled residual dipolar terms remain and lead to the decay of these strongly coupled (broad) signals, leaving only signals arising from “weakly coupled” crystallites, which have narrow lines. This yields spectra with less dipolar broadening and thus resolution enhancement. This has allowed, for example, the methylene resonance  $[\text{MCH}_2]$  in  $[(\text{=SiO})\text{Mo}(\text{=NAr})(\text{=CH}t\text{Bu})(\text{CH}_2t\text{Bu})]$  and  $[(\text{=SiO})\text{Re}(\text{=C}t\text{Bu})(\text{=CH}t\text{Bu})(\text{CH}_2t\text{Bu})]$  to be directly observed, whereas this signal



**Scheme 2** Pulse sequence for various NMR experiments presented here to solve chemical problems in the solid state. (a)  $^1\text{H}$  delayed acquisition experiment. (b)  $^1\text{H}$ - $^1\text{H}$  Constant Time experiment to obtain highly resolved  $^1\text{H}$  spectra. (c) General scheme of  $^1\text{H}$ - $^1\text{H}$  Double Quantum experiment to detect proton connectivity. (d) General scheme of  $^1\text{H}$ - $^1\text{H}$  Triple Quantum experiment to detect proton connectivity. (e)  $^{13}\text{C}$  CP MAS experiment. (f)  $^1\text{H}$ - $^{13}\text{C}$  HETCOR experiment to probe through space nuclei connectivity. (g)  $^1\text{H}$ - $^{13}\text{C}$  solid state  $J$ -resolved experiment. Dark grey denotes heteronuclear decoupling while light grey denotes MAS alone or MAS combined with homonuclear decoupling.

was buried under the large  $t\text{Bu}$  peaks when using standard  $^1\text{H}$  single pulse techniques. The resolution can be further improved by using the constant time experiment,<sup>21</sup> a 2D NMR sequence in which acquisition of the signal in  $t_2$  starts at a constant time  $T$  after the initial  $90^\circ$  proton pulse; a  $180^\circ$  proton pulse is shifted from the middle to the end of the constant time interval (Scheme 2b) and allows spectra in  $\omega_1$  to be completely free of

residual homogeneous dipolar broadening. Application of this technique to the two examples cited above yields a dramatic resolution enhancement illustrated for  $[(\equiv\text{SiO})\text{Mo}(\equiv\text{NAr})(=\text{CH}t\text{Bu})(\text{CH}_2t\text{Bu})]$  in Fig. 2c.<sup>17</sup>

In summary, these simple delayed acquisition techniques can dramatically improve resolution, and can be used to extract significantly more information from the  $^1\text{H}$  MAS spectrum and provide a more precise molecular understanding of the well-defined heterogeneous catalysts.

#### 4. Homonuclear connectivities and proximities on surfaces

As in solution state NMR, the use of two-dimensional (2D) NMR is often an essential step in order to make unequivocal assignments. Taking the advantage of dipolar couplings (through space), we illustrate in the following how it is possible to obtain correlations between neighboring protons.

Two dimensional (2D) multiple quantum (MQ)  $^1\text{H}$ - $^1\text{H}$  spectroscopy is a powerful technique to investigate structural information inherent to  $^1\text{H}$ - $^1\text{H}$  dipolar coupling.<sup>15,22</sup> This type of spectrum can be obtained by using the following NMR pulse sequence illustrated in Scheme 2: excitation of double quantum coherences using a recoupling sequence,  $t_1$  evolution, reconversion before detection (Scheme 2c). Evolution of the DQ coherences is obtained in the indirect dimension ( $F_1$ ) at a frequency which corresponds to the sum of the two individual single-quantum frequencies of the two coupled (or spatially close) protons ( $F_2$ ) (Fig. 3).

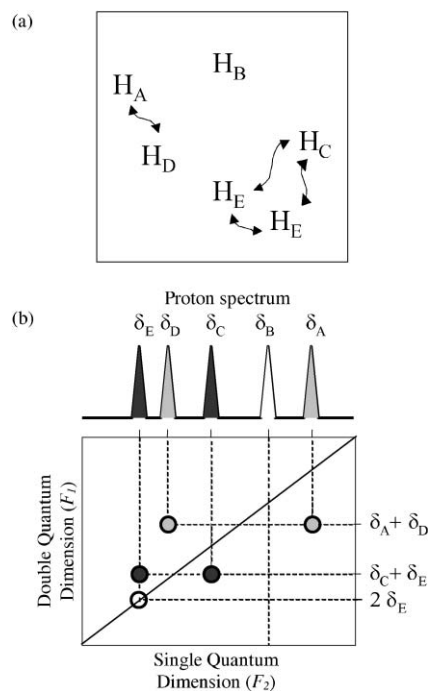


**Fig. 3** (a) Schematic representation of protons interacting or not. (b) Corresponding proton and two-dimensional Double Quantum (DQ) spectra: the DQ frequency in the  $F_1$  dimension corresponds to the sum of the two single quantum frequencies of the two coupled protons and correlates in the  $F_2$  dimension with the two corresponding proton resonances.

This has notably been used to characterize the active sites of supported metal hydrides, which show unusual properties in alkane activation and conversion processes.<sup>23</sup> For instance, the silica supported zirconium hydrides  $[(\equiv\text{SiO})_x\text{Zr}(\text{H})_{4-x}]$  ( $x = 2$  or 3) have been shown to be composed in this way of a mono- and bis(hydride) surface species, noted  $[(\equiv\text{SiO})_3\text{ZrH}]$  and  $[(\equiv\text{SiO})_2\text{ZrH}_2]$ , respectively, which display two distinctive peaks at 10.1 and 12.1 ppm in the  $^1\text{H}$  single pulse spectrum (Fig. 4a).<sup>24,25</sup> While the longitudinal relaxation time  $T_1$ , which is very different for the peaks at 10.1 ppm ( $T_1 \sim 10$  s) and 12.1 ppm ( $T_1 \sim 0.5$  s), is consistent with two protons in totally different environments (the latter proton relaxes quickly by an efficient dipolar relaxation pathway, suggesting the proximity of other dipoles, while the former proton is more isolated), the 2D  $^1\text{H}$ - $^1\text{H}$  DQ NMR spectrum of Fig. 4 was necessary to assign unambiguously these two protons.<sup>25</sup> A strong autocorrelation for the  $^1\text{H}$  resonance at 12.1 ppm ( $\omega_2$ ) in the double quantum dimension (at a frequency  $\omega_1$  of 24.2 ppm) indicates a close proximity between the two protons in the same environment, hence a dihydride  $[(\equiv\text{SiO})_2\text{ZrH}_2]$ . The proton at

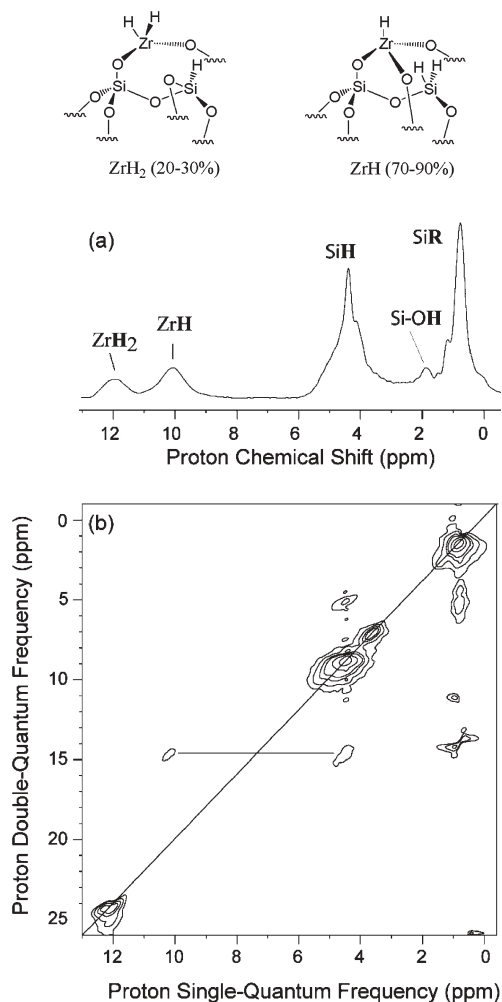


**Fig. 4** Molecular structure of zirconium hydrides complexes  $[(\equiv\text{SiO})_x\text{Zr}(\text{H})_{4-x}]$ <sup>25</sup> ( $x = 2, 3$ ) and their  $^1\text{H}$  MAS spectra. (a) One dimensional single pulse  $^1\text{H}$  spectrum. (b)  $^1\text{H}$  Double Quantum (DQ) correlation spectrum. Reproduced with permission from the authors.<sup>25</sup>

10.1 ppm has no autocorrelation peak (which would appear at 20.2 ppm) and presents a weak correlation at 14.5 ppm in the  $\omega_1$  dimension, consistent with a monohydride species  $[(\equiv\text{SiO})_3\text{ZrH}]$  in close proximity with a Si-H (4.4 ppm) (Fig. 4).

In another example, a triple-quantum spectrum (TQ) was used to discriminate the different protons of the N-containing ligand for  $[(\equiv\text{SiO})_2\text{Ta}(\text{=NH})(\text{NH}_2)(\text{NH}_3)]$  (Fig. 5).<sup>26</sup> While the imido moiety  $[\text{Ta}(\text{=NH})]$  does not give auto correlation in either the DQ or TQ dimension, the  $[\text{Ta}(\text{NH}_2)]$  amido protons at 4.3 ppm give autocorrelation at 8.6 ppm in the DQ

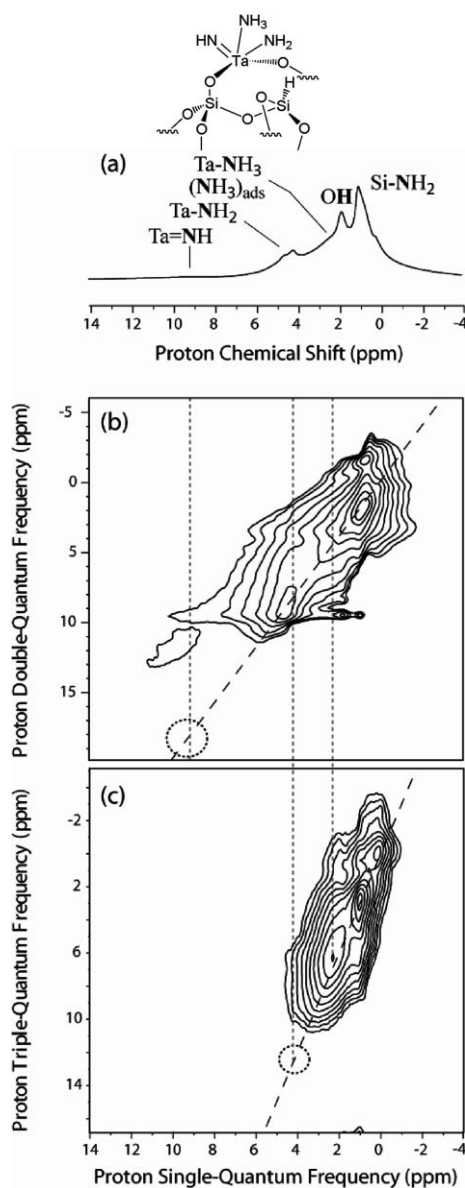


**Fig. 5** Molecular structure of tantalum imido amido amino complexes  $[(\equiv\text{SiO})_2\text{Ta}(\text{=NH})(\text{NH}_2)(\text{NH}_3)]$ <sup>26a</sup> and their  $^1\text{H}$  MAS spectra. (a) One dimensional single pulse  $^1\text{H}$  spectrum. (b)  $^1\text{H}$  Double Quantum (DQ) correlation spectrum. (c)  $^1\text{H}$  Triple Quantum (TQ) correlation spectrum. The dotted gray lines correspond to the resonances of the tantalum NH,  $\text{NH}_2$  and  $\text{NH}_3$  protons. The dotted circles underline the absence of autocorrelation peaks for the imido NH proton in the DQ spectrum (b), for the amido  $\text{NH}_2$  proton in the triple quantum spectrum (c). Adapted with permission from the authors.<sup>26a</sup>

dimension *but not in the TQ dimension* and the  $[\text{Ta}(\text{NH}_3)]$  ammonia adduct protons at 2.2 ppm correlate with themselves at 6.6 ppm in the TQ dimension. The TQ spectrum was obtained by adding a  $90^\circ$  proton pulse before the DQ excitation blocks as described above followed by  $t_1$  evolution under homonuclear decoupling, reconversion, Z-filter and proton detection (Scheme 2d).<sup>27,28</sup>

In summary, these examples illustrate very nicely how proton multiple-quantum spectra can be used in heterogeneous catalysis or disordered materials<sup>28,29</sup> in order to give very simple and clear cut answers to otherwise very difficult characterisation challenges.

## 5. Heteronuclear connectivities and proximities on surfaces

2D heteronuclear correlation spectroscopy (HETCOR) can be used to ascertain spectral assignments by correlating the chemical shifts of protons with another nucleus X. The heteronucleus is often carbon-13, but can equally well be  $^{15}\text{N}$ ,  $^{29}\text{Si}$  or  $^{31}\text{P}$ .<sup>30</sup> The pulse sequence for solid state MAS  $^1\text{H}$ - $^{13}\text{C}$  HETCOR is shown in Scheme 2e. The NMR pulse sequence consists first of a  $90^\circ$  proton pulse, which rotates the proton magnetization into the  $xy$  plane. Then it evolves during  $t_1$  and is subsequently transferred to the  $^{13}\text{C}$  spin *via* a CP step. Detection of carbon magnetization is then achieved under proton decoupling. A 2D Fourier transform yields through space correlations between neighbouring proton (in  $\omega_1$ ) and carbon (in  $\omega_2$ ) spins.

Note that polarisation transfer is achieved by through space dipolar interactions. For short contact time (*e.g.* 0.5–1 ms), this process can be quite selective, and thus pairs of attached  $^1\text{H}$ - $^{13}\text{C}$  spins can be selectively detected.<sup>12b</sup> For instance, the 2D HETCOR spectra of  $[(\text{=SiO})\text{Re}(=\text{*C}t\text{Bu})(=\text{*CH}t\text{Bu})(\text{*CH}_2t\text{Bu})]^{12b}$  in a *syn* : *anti* 1 : 1 mixture (depending of the orientation of the alkylidene towards the alkylidyne) recorded with a short contact time of 0.5 ms showed correlations between directly bonded proton and carbon (Fig. 6). In this case, the  $^{13}\text{C}$  labelled methylene carbon  $[\text{Re}(\text{CH}_2t\text{Bu})]$  at 44 ppm is correlated with the two diastereotopic methylene protons of the neopentyl group  $[\text{Re}(\text{CH}_2t\text{Bu})]$  at 2.6 and 3.0 ppm, allowing a detailed understanding of the surface species. Moreover, 2D HETCOR NMR can be used to distinguish between a mixture of surface species, for example the  $^1\text{H}$ - $^{13}\text{C}$  correlations at 11.0 ppm ( $^1\text{H}$ )-247 ppm ( $^{13}\text{C}$ ) and 12.5 ppm ( $^1\text{H}$ )-257 ppm ( $^{13}\text{C}$ ) allow the identification of two isomers, the *syn* and *anti* rotamers, respectively. Additionally, the use of a longer CP time (*e.g.* 10 ms) allowed extra correlations to be observed, which are due to more remote carbon–proton pairs. These long range interactions help to obtain a complete assignment of the carbon and  $^1\text{H}$  spectra. For instance, a cross peak between carbon at 44 ppm and the alkylidene proton  $[\text{Re}(=\text{CH}t\text{Bu})]$  at 11.1 ppm corresponds to the interaction between this proton and the quaternary carbon of the neopentylidene group,  $[\text{Re}(=\text{CHCMe}_3)]$ .

$^1\text{H}$ -X 2D HETCOR NMR spectroscopy has now become a routine method for unequivocal assignments of surface complexes, from well-defined alkylidene to more complex systems such as Zr carboxylate species obtained by treatment

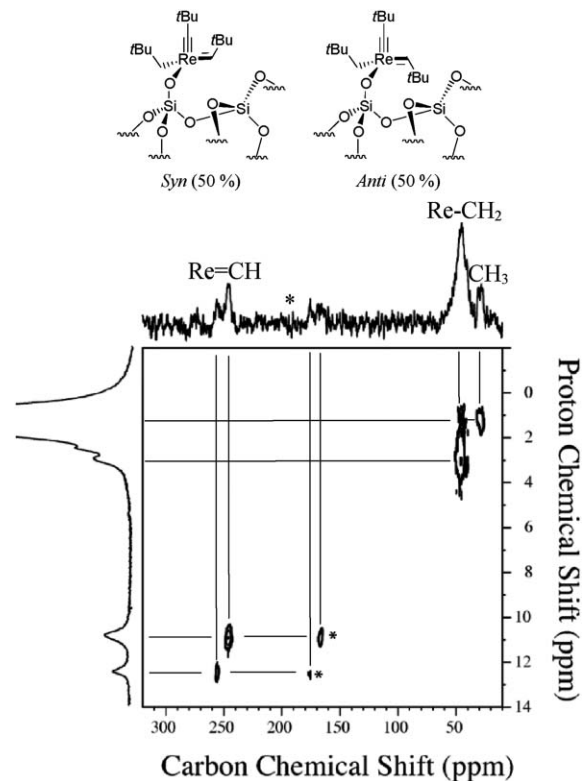


**Fig. 6** Molecular structure and  $^1\text{H}$ - $^{13}\text{C}$  HETCOR spectra of  $^{13}\text{C}$  labelled  $[(\text{=SiO})\text{Re}(=\text{*C}t\text{Bu})(=\text{*CH}t\text{Bu})(\text{*CH}_2t\text{Bu})]^{12b}$  as a *syn* : *anti* 1 : 1 mixture recorded at MAS frequency of 10 kHz and CP step of 0.5 ms. Top:  $^{13}\text{C}$  CP MAS spectra. Left: zoom in the  $^1\text{H}$  single pulse spectra. Asterisk (\*) denotes the correlation peaks with spinning side bands. Adapted with permission from the authors.<sup>12b</sup>

of surface hydrides with  $\text{CO}_2$ <sup>25</sup> or methyltrioxorhenium on inorganic support.<sup>31</sup> Similarly,  $^1\text{H}$ - $^{29}\text{Si}$  HETCOR helps the assignment of silane groups on  $[(\text{=SiO})_x\text{Si}(\text{H})_{4-x}]^{25}$  ( $x = 2,3$ ), of allylic functionalities in the pores of mesoporous materials<sup>32</sup> and also the understanding of the surface and silicon network of mesoporous silicas.<sup>33</sup>

*Improving resolution of 2D HETCOR spectra.* When necessary, the resolution of the HETCOR spectra can be improved by applying homonuclear decoupling for example for  $[(\text{=SiO})_2\text{Ta}(=\text{NH})(\text{NH}_2)(\text{NH}_3)]^{26}$  or with a constant-time (CT) period in the  $^1\text{H}$  dimension, for example for  $[(\text{=SiO})\text{Mo}(=\text{NAr})(=\text{CH}t\text{Bu})(\text{CH}_2t\text{Bu})]^{17}$ . In the latter case, the CT HETCOR experiment allowed distinction between direct and indirect correlations. This distinction was not possible on the basis of the HETCOR experiment itself and thus the CT HETCOR experiment provides a significant gain in information.

## 6. Determination of the local geometry of surface species by measuring scalar $J$ coupling constants

Distinction of different types of perhydrocarbyl ligands, such as alkyl  $[\text{M}(\text{CH}_2\text{R})]$ , alkylidene  $[\text{M}(=\text{CRH})]$  and alkylidyne  $[\text{M}(=\text{CR})]$  ligands is possible if one could access the scalar  $^1J_{\text{C-H}}$  coupling constants, which are directly related to the carbon hybridization,  $^1J_{\text{C-H}} = 500/(n + 1)$  for  $\text{sp}^n$ . While

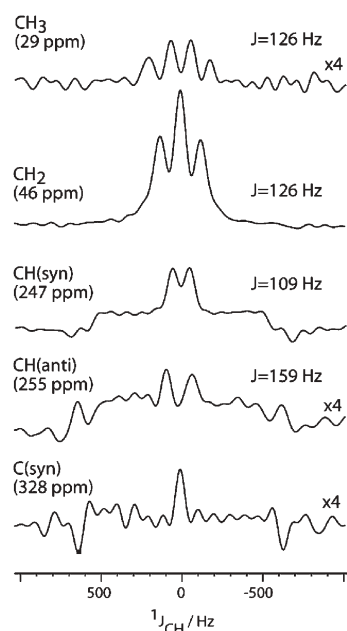
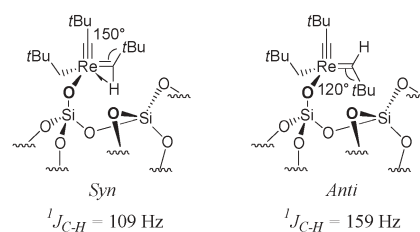


**Fig. 7** Traces extracted along the  $\omega_1$  dimension of the 2D  $J$ -resolved spectrum of  $[(\equiv\text{SiO})\text{Re}(\equiv\text{C}t\text{Bu})(=\text{CH}t\text{Bu})(\text{CH}_2t\text{Bu})]^{35}$  (*syn/anti* ratio 1 : 1) at different carbon chemical shift frequencies. Reproduced with permission from the authors.<sup>35</sup>

heteronuclear  $J$  resolved spectroscopy is one of the most basic techniques available in solution NMR,<sup>3c</sup> it remains very challenging in solid state NMR. Indeed, the size of the C–H scalar interactions – in the range of 100 Hz – is much smaller than that of the anisotropic interactions such as the dipolar couplings or the chemical shift anisotropies (a few kHz) and is comparable to typical linewidths. Nevertheless, using homonuclear decoupling schemes,<sup>18,34</sup> it has been recently possible to remove the anisotropic interactions so as to observe the heteronuclear  $J_{\text{C-H}}$  coupling constants in solids.<sup>34</sup>

Applying the solid state  $J$ -resolved experiment to  $[(\equiv\text{SiO})\text{Re}(\equiv\text{C}t\text{Bu})(=\text{CH}t\text{Bu})(\text{CH}_2t\text{Bu})]^{35}$  as illustrated in Fig. 6 has therefore allowed carbons to be distinguished according to their proton multiplicities, and not solely from chemical shift differences.<sup>36</sup> The pulse sequence (Scheme 2f) starts by a cross polarization step to transfer the proton magnetization to the carbon nuclei. During the evolution period  $t_1$ , the  $^1\text{H}$  proton dipolar couplings are removed by homonuclear decoupling, whereas the remaining inhomogeneous interactions, the chemical shift and the heteronuclear dipolar couplings, are averaged out by magic angle spinning to



**Scheme 3**

their isotropic part, leaving only the isotropic chemical shift and the heteronuclear scalar couplings. The  $180^\circ$  carbon pulse, applied in the middle of  $t_1$ , refocuses the chemical shift, but not the scalar coupling so that the carbon magnetization will be only modulated during  $t_1$  by the heteronuclear  $^1J_{\text{C-H}}$  couplings. A 2D Fourier transform yields correlation between heteronuclear  $J$  multiplet structures (in  $\omega_1$ ) and carbon chemical shifts (in  $\omega_2$ ). For instance, using this approach on  $[(\equiv\text{SiO})\text{Re}(\equiv\text{C}t\text{Bu})(=\text{CH}t\text{Bu})(\text{CH}_2t\text{Bu})]^{35}$  selectively labeled on the carbon directly bonded to Re, it was possible to distinguish the neopentyl,  $[\text{Re}(\text{CH}_2t\text{Bu})]$ , the neopentylidene  $[\text{Re}(\equiv\text{CH}t\text{Bu})]$  and neopentylidyne  $[\text{Re}(\equiv\text{C}t\text{Bu})]$  carbon resonances as triplet, doublet and singlet, respectively in the  $\omega_1$  scalar  $^1J_{\text{C-H}}$  coupling dimension (Fig. 7).

Moreover, it was also possible to characterize the two rotamers of  $[(\equiv\text{SiO})\text{Re}(\equiv\text{C}t\text{Bu})(=\text{CH}t\text{Bu})(\text{CH}_2t\text{Bu})]$ : the alkylidenes at 247 and 255 ppm have coupling constants of 109 and 159 Hz, in agreement with their assignments to *syn* and *anti* rotamers, respectively. In fact, the small  $^1J_{\text{C-H}}$  coupling constant of 109 Hz for the *syn* rotamer indicates the presence of an agostic interaction,<sup>37</sup> which elongates the C–H bond and decreases the  $^1J_{\text{C-H}}$  coupling constant.

This technique has now been applied to characterize a wide variety of surface complexes:  $[(\equiv\text{SiO})\text{M}(\equiv\text{CH}_2t\text{Bu})_3]$  ( $\text{M} = \text{Zr}, \text{Hf}$ ),<sup>38</sup>  $[(\equiv\text{SiO})\text{M}(\text{ER})(=\text{CH}t\text{Bu})(\text{R}')]$  ( $\text{M} = \text{Ta}$ ,<sup>39</sup>  $\text{ER} = \text{R}' = \text{CH}_2t\text{Bu}$ ;  $\text{M} = \text{Mo}$ ,<sup>40</sup>  $\text{ER} = \text{NAr}$  ( $\text{Ar} = 2,6\text{-}i\text{Pr}_2\text{C}_6\text{H}_3$ ),  $\text{R}' = \text{CH}_2t\text{Bu}$ ;  $\text{M} = \text{Mo}$ ,<sup>40</sup>  $\text{ER} = \text{NAr}$ ,  $\text{R}' = \text{NPh}_2$ ;  $\text{M} = \text{Mo}$ ,<sup>40</sup>  $\text{ER} = \text{NAr}$ ,  $\text{R}' = \text{pyrrolyl}$ ), and  $[(\equiv\text{SiO})\text{W}(\equiv\text{C}t\text{Bu})(=\text{CH}t\text{Bu})_2]$ .<sup>41</sup>

In the case of Mo imido alkylidene species, the low  $^1J_{\text{C-H}}$  values allow their unequivocal assignments to *syn* complexes (Table 1). Furthermore, it has been shown in molecular organometallic chemistry that the  $^1J_{\text{C-H}}$  coupling constants can be directly used to evaluate the M–C–C bond angles in a range of model alkylidene complexes.<sup>42</sup> In this way, M–C–C bond angles can be evaluated, which is not possible with X-Ray based techniques. This is illustrated in Scheme 3 with one example,  $[(\equiv\text{SiO})\text{Re}(\equiv\text{C}t\text{Bu})(=\text{CH}t\text{Bu})(\text{CH}_2t\text{Bu})]$ .

**Table 1** Isotropic chemical shift ( $\delta_{\text{iso}}$ ), scalar  $J$  coupling constants ( $^1J_{\text{C-H}}$ ) of  $\alpha$ -carbon bonded to the metal centre of various well defined silica complexes. An estimated M–C–C bond angle<sup>42</sup> in degrees is given for alkylidene carbons  $[\text{M}]=\text{CH}$

Complexes	CH <sub>2</sub>		CH		M–C–C <sup>o</sup>
	$\delta_{\text{iso}}/\text{ppm}$	$^1J_{\text{C-H}}/\text{Hz}$	$\delta_{\text{iso}}/\text{ppm}$	$^1J_{\text{C-H}}/\text{Hz}$	
$[(\equiv\text{SiO})\text{Ta}(\equiv\text{CH}t\text{Bu})(\text{CH}_2t\text{Bu})_2]^{39}$	95	125	247	80	170
$[(\equiv\text{SiO})\text{W}(\equiv\text{C}t\text{Bu})(\text{CH}_2t\text{Bu})_2]^{41}$	95	110	—	—	—
$[(\equiv\text{SiO})\text{Mo}(\equiv\text{NAr})(=\text{CH}t\text{Bu})(\text{CH}_2t\text{Bu})]^{40}$	56	124	279	110	150
$[(\equiv\text{SiO})\text{Mo}(\equiv\text{NAr})(=\text{CH}t\text{Bu})(\text{NPh}_2)]^{40}$	—	—	288	107	150
$[(\equiv\text{SiO})\text{Mo}(\equiv\text{NAr})(=\text{CH}t\text{Bu})(\text{NC}_4\text{H}_9)]^{40}$	—	—	285	109	150

## Conclusions

High resolution two-dimensional  $^1\text{H}$ - $^1\text{H}$  and  $^1\text{H}$ - $\text{X}$  ( $\text{X} = ^{13}\text{C}$ ,  $^{15}\text{N}$ ...) NMR provide a range of exquisitely precise tools to characterize well-defined active sites in heterogeneous catalysis. Implementation of high resolution and 2D solid state NMR techniques has already helped to identify surface structures at a molecular level, which is key to implementing structure–reactivity relationships and rational developments in heterogeneous catalysis. It is clear that these methods also have the potential for extensive further developments and applications, for example towards understanding more complex systems (complex oxide materials, active sites with paramagnetic or quadrupolar centres), probing the dynamics of surface species (access to mobility of active sites), and to monitor the active sites as a function of time (*in operando* or in conditions close to those used in catalytic tests).

## Acknowledgements

F. B. is grateful to the French ministry of education, research and technology (MENRT) for a graduate fellowship. C. C. is grateful to ANR for a young investigator grant (ANR JC05\_46372). We are indebted to all co-workers whose names are listed within the references and the CNRS, ESCPE Lyon, ENS Lyon, MENRT, all our past and present industrial partners for financial supports. We are indebted to the European Large Scale Facility for NMR in Lyon, France for spectrometer time.

## References

- (a) C. Copéret, M. Chabanas, R. Petroff Saint-Arroman and J.-M. Basset, *Angew. Chem., Int. Ed.*, 2003, **42**, 156; (b) C. Copéret, *New J. Chem.*, 2004, **28**, 1; (c) C. Copéret, *Dalton Trans.*, 2007, DOI: 10.1039/b713314f, in press.
- (a) J. C. Fierro-Gonzalez, S. Kuba, Y. L. Hao and B. C. Gates, *J. Phys. Chem. B*, 2006, **110**, 13326; (b) C. Bonhomme, C. Coelho, N. Baccile, C. Gervais, T. Azais and F. Babonneau, *Acc. Chem. Res.*, 2007, **40**, 738.
- (a) K. Schmidt-Rohr and H. W. Spiess, *Multidimensional Solid-state NMR and Polymers*, Academic Press, London, 1994; (b) M. Mehring, *Principles of High Resolution NMR in Solids*, Springer, Berlin, 1983; (c) R. R. Ernst, M. Bodenhausen and A. Wokaun, *Principles of Nuclear Magnetic Resonance in One and Two Dimensions*, Oxford Science, N. York, 1987.
- E. R. Andrew, A. Bradbury and R. G. Eades, *Nature*, 1959, **183**, 1802.
- I. Lowe, *Phys. Rev. Lett.*, 1959, **2**, 285.
- (a) S. R. Hartmann and E. L. Hahn, *Phys. Rev.*, 1962, **128**, 2042; (b) A. Pines, M. G. Gibby and J. S. Waugh, *J. Chem. Phys.*, 1973, **59**, 569; (c) J. Schaefer and E. O. Stejskal, *J. Am. Chem. Soc.*, 1976, **98**, 1031.
- L. Reven, *J. Mol. Catal.*, 1994, **86**, 447.
- (a) W. Kolodziejski and J. Klinowski, *Chem. Rev.*, 2002, **102**, 613; (b) E. O. Stejskal and J. D. Memory, *High Resolution NMR in the Solid State. Fundamentals of CP/MAS*, Oxford University Press, Oxford, 1994.
- F. Lopez-Ortiz and R. J. Carbajo, *Curr. Org. Chem.*, 1998, **2**, 97.
- E. Vinogradov, P. K. Madhu and S. Vega, *Top. Curr. Chem.*, 2004, **246**, 33.
- P. Hodgkinson, *Prog. Nucl. Magn. Reson. Spectrosc.*, 2005, **46**, 197.
- (a) M. Chabanas, A. Baudouin, C. Copéret, J.-M. Basset, W. Lukens, A. Lesage, S. Hediger and L. Emsley, *J. Am. Chem. Soc.*, 2003, **125**, 492; (b) T. J. Marks, *Acc. Chem. Res.*, 1992, **25**, 57.
- (a) G. Engelhardt, in *Handbook of Heterogeneous Catalysis*, ed. G. Ertl, H. Knözinger, and J. Weitkamp, WILEY-VCH, Weinheim, 1997; (b) A. Sebald, in *Advanced applications of NMR to Organometallic Chemistry*, ed. M. Gielen, R. Willem, and B. Wrackmeyer, Chichester, 1996; (c) S. Aime, W. Dastrù, R. Gobetto and G. E. Hawkes, in *Advanced applications of NMR to Organometallic Chemistry*, ed. M. Gielen, R. Willem, and B. Wrackmeyer, Chichester, 1996; (d) M. Hunger and J. Weitkamp, *Angew. Chem., Int. Ed.*, 2001, **40**, 2954.
- A. Samoson, T. Tuherm and Z. Gan, *Solid State Nucl. Magn. Reson.*, 2001, **20**, 130.
- S. P. Brown and H. W. Spiess, *Chem. Rev.*, 2001, **101**, 4125.
- F. Blanc, C. Copéret, J. Thivolle-Cazat, J.-M. Basset, A. Lesage, L. Emsley, A. Sinha and R. R. Schrock, *Angew. Chem., Int. Ed.*, 2006, **45**, 1216.
- F. Blanc, C. Copéret, J. Thivolle-Cazat, J.-M. Basset, A. Lesage, L. Emsley, A. Sinha and R. R. Schrock, *Inorg. Chem.*, 2006, **45**, 9587.
- (a) D. Sakellariou, A. Lesage, P. Hodgkinson and L. Emsley, *Chem. Phys. Lett.*, 2000, **319**, 253; (b) A. Lesage, D. Sakellariou, S. Hediger, B. Elena, P. Charmont, S. Steuernagel and L. Emsley, *J. Magn. Reson.*, 2003, **163**, 105.
- B. Elena, G. de Paepe and L. Emsley, *Chem. Phys. Lett.*, 2004, **398**, 532.
- S. Ding and C. A. McDowell, *J. Magn. Reson., Ser. A*, 1994, **111**, 212.
- A. Lesage, L. Duma, D. Sakellariou and L. Emsley, *J. Am. Chem. Soc.*, 2001, **123**, 5747.
- (a) H. Geen, J. J. Titman, J. Gottwald and H. W. Spiess, *Chem. Phys. Lett.*, 1994, **227**, 79; (b) S. P. Brown, *Prog. Nucl. Magn. Reson. Spectrosc.*, 2007, **50**, 199.
- J. M. Basset, C. Copéret, D. Soulivong, M. Taoufik and J. Thivolle-Cazat, *Angew. Chem., Int. Ed.*, 2006, **45**, 6082.
- V. A. Zakharov and Y. A. Ryndin, *J. Mol. Catal.*, 1989, **56**, 183.
- F. Rataboul, A. Baudouin, C. Thieuleux, L. Veyre, C. Copéret, J. Thivolle-Cazat, J.-M. Basset, A. Lesage and L. Emsley, *J. Am. Chem. Soc.*, 2004, **126**, 12541.
- (a) P. Avenier, A. Lesage, M. Taoufik, A. Baudouin, A. De Mallmann, S. Fiddy, M. Vautier, L. Veyre, J. M. Basset, L. Emsley and E. A. Quadrelli, *J. Am. Chem. Soc.*, 2007, **129**, 176; (b) P. Avenier, M. Taoufik, A. Lesage, A. Baudouin, X. Solans-Monfort, A. De Mallmann, L. Veyre, J. M. Basset, O. Eisenstein, L. Emsley and E. A. Quadrelli, *Science*, 2007, **317**, 1056.
- (a) I. Schnell and H. W. Spiess, *J. Magn. Reson.*, 2001, **151**, 153; (b) I. Schnell, S. P. Brown, H. Y. Low, H. Ishida and H. W. Spiess, *J. Am. Chem. Soc.*, 1998, **120**, 11784; (c) U. Friedrich, I. Schnell, D. E. Demco and H. W. Spiess, *Chem. Phys. Lett.*, 1998, **285**, 49.
- D. F. Shantz, J. S. auf der Gunne, H. Koller and R. F. Lobo, *J. Am. Chem. Soc.*, 2000, **122**, 6659.
- (a) F. Babonneau, C. Bonhomme, C. Gervais and J. Maquet, *J. Sol-Gel Sci. Technol.*, 2004, **31**, 9; (b) K. Saalwachter, M. Krause and W. Gronski, *Chem. Mater.*, 2004, **16**, 4071.
- D. M. Burum, in *Encyclopedia of Nuclear Magnetic Resonance*, ed. D. M. Grant and R. K. Harris, Wiley, Chichester, 1997.
- (a) A. Salameh, J. Joubert, A. Baudouin, W. Lukens, F. Delbecq, P. Sautet, J.-M. Basset and C. Copéret, *Angew. Chem., Int. Ed.*, 2007, **46**, 3870; (b) A. W. Moses, C. Raab, R. C. Nelson, H. D. Leifeste, N. A. Ramsahye, S. Chattopadhyay, J. Eckert, B. F. Chmelka and S. L. Scott, *J. Am. Chem. Soc.*, 2007, **129**, 8912.
- J. Trebosc, J. W. Wiench, S. Huh, V. S. Y. Lin and M. Pruski, *J. Am. Chem. Soc.*, 2005, **127**, 7587.
- S. C. Christiansen, D. Y. Zhao, M. T. Janicke, C. C. Landry, G. D. Stucky and B. F. Chmelka, *J. Am. Chem. Soc.*, 2001, **123**, 4519.
- A. Lesage, S. Steuernagel and L. Emsley, *J. Am. Chem. Soc.*, 1998, **120**, 7095.
- A. Lesage, L. Emsley, M. Chabanas, C. Copéret and J.-M. Basset, *Angew. Chem., Int. Ed.*, 2002, **41**, 4535.
- R. R. Schrock, *Chem. Rev.*, 2002, **102**, 145.
- M. Brookhart and M. L. H. Green, *J. Organomet. Chem.*, 1983, **250**, 395.
- G. Tosin, C. C. Santini, M. Taoufik, A. De Mallmann and J.-M. Basset, *Organometallics*, 2006, **25**, 3324.



- 39 E. L. Le Roux, M. Chabanas, A. Baudouin, A. de Mallmann, C. Copéret, E. A. Quadrelli, J. Thivolle-Cazat, J.-M. Basset, W. Lukens, A. Lesage, L. Emsley and G. J. Sunley, *J. Am. Chem. Soc.*, 2004, **126**, 13391.
- 40 F. Blanc, C. Copéret, A. Lesage and L. Emsley, unpublished results.

- 41 E. Le Roux, M. Taoufik, M. Chabanas, D. Alcor, A. Baudouin, C. Copéret, J. Thivolle-Cazat, J.-M. Basset, A. Lesage, S. Hediger and L. Emsley, *Organometallics*, 2005, **24**, 4274.
- 42 (a) R. R. Schrock, *Acc. Chem. Res.*, 1979, **12**, 98; (b) W. A. Nugent and J. M. Mayer, *Metal-Ligand Multiple Bond*, Wiley, N. York, 1988.



Save valuable time searching for that elusive piece of vital chemical information.

Let us do it for you at the Library and Information Centre of the RSC.

We are your chemical information support, providing:

- Chemical enquiry helpdesk
- Remote access chemical information resources
- Speedy response
- Expert chemical information specialist staff

Tap into the foremost source of chemical knowledge in Europe and send your enquiries to

**library@rsc.org**

12120515

RSCPublishing

**www.rsc.org/library**